Longer survival of Helicobacter pylori positive gastric cancer patients is associated with a more active T cell immune response as revealed by single-cell sequencing

Yun Chen (chenyun@njmu.edu.cn)
Nanjing Medical University
Caiwang Yan
Nanjing Medical University
Shujing Shi
Nanjing Medical University
Chang Zheng
Medical School of Nanjing University
Chuanli Ren
Clinical Medical College of Yangzhou University
Lijun Bian
Nanjing Medical University
Yuanliang Gu
Nanjing Medical University
Deyuan Kong
Nanjing Medical University
Qiang She
the Affiliated Hospital of Yangzhou University, Yangzhou University
Bin Deng
the Affiliated Hospital of Yangzhou University, Yangzhou University
Yanbing Ding
the Affiliated Hospital of Yangzhou University, Yangzhou University
Jinfei Chen
the First Affiliated Hospital of Wenzhou Medical University
Runqiu Jiang
Medical School of Nanjing University

Research Article

Keywords: gastric cancer, Helicobacter pylori, immune microenvironment, survival

Posted Date: January 31st, 2022

DOI: https://doi.org/10.21203/rs.3.rs-1302906/v1

Abstract

Background: The effect of *Helicobacter pylori* (*H. pylori*) status on survival for gastric cancer remains unclear. We aimed to elucidate the molecular heterogeneity of tumour-infiltrating T cells in gastric cancer with different *H. pylori* infection status.

Methods: We conducted a prognostic analysis of 488 gastric cancer patients and performed single-cell RNA sequencing (scRNA-seq) analysis on 18,717 T cells from 6 tumour samples with or without *H. pylori* infection. Analysis results were validated using histological assays and bulk transcriptomic datasets.

Results: We confirmed that gastric cancer patients with *H. pylori* infection had a significantly longer survival time compared to patients with negative *H. pylori* status (HR=0.74, 95% CI=0.55-0.99, *P*= 0.045). After unsupervised re-clustering of T cells based on scRNA-seq data, we identified ten $CD4^+$ and twelve $CD8^+$ clusters. Among them, four clusters in $CD8^+$ T cells appeared to exhibit distinct distributions with different *H. pylori* infection status. One subgroup marked by *CXCL13*, which contained mostly cells of *H. pylori* infection and expressed high levels of *IFNG*, *GZMB* and low level of *PDCD1*, was activated by *TNFRSF1A-TNF* interaction. The developed gene signature was significantly associated with improved patient survival in gastric cancer. The other subgroup specifically expressed immune suppression-related genes *AREG* and *PTGER2*, was almost exclusively populated with cells without *H. pylori* infection. High *PTGER2* expression was significantly associated with worse prognosis with high CD8 expression.

Conclusion: Our results shed light into the mechanisms underlying the target cell dependent T cell responses induced by *H. pylori*, which will provide assistance for precision treatment and prognosis.

Introduction

Helicobacter pylori (*H. pylori*) has been classified as a Group I carcinogenic pathogen (1) because its infection was epidemically and etiological seriously associated with oncogenesis of gastric cancer (2). Hence, it is well accepted that eliminating *H. pylori* infection is an effective way in gastric cancer prevention. However, gastric cancer develops through a multistep process, whether *H. pylori* plays the carcinogenic role among the whole progression is controversial. Masanori summarized that *H. pylori* is not required for the maintenance of a neoplastic phenotype in established cancer cells through a hit-and-run mechanism in which pro-oncogenic actions are successively taken over by a series of genetic and/or epigenetic alterations compiled in cancer-predisposing cells during long-standing infection with *H. pylori* (3). In addition, it is noteworthy that eradication of *H. pylori* appears to be ineffective for the prevention of gastric cancer in two trials that included subjects with precancerous lesions, including low to high-grade dysplasia at baseline (4, 5). This indicates that eradication of *H. pylori* before the development of precancerous lesions offers better protection against gastric cancer. It seems one of the reason is that an elevated pH caused by *H. pylori* facilitates the intrusion of oral or intestinal bacteria into the stomach that may additionally contribute to the development of mucosal lesions (6), while the damaged environment is no longer suitable for *H. pylori* survival, especially in gastric cancer (7).

The gut microbiota and the immune system have coevolved and affect each other directly and via metabolic crosstalk (8). For example, Beura and colleagues (9) discovered that wild mice, pet store mice and adult humans, but neither “clean” laboratory mice nor human neonates, have a highly differentiated memory $CD8^+$ T-cell compartment in blood. Especially, multiple studies have provided strong evidence that immunotherapy may be an effective treatment for cancer if tumor microenvironment (TME) components are properly understood and judiciously targeted (10). Basically, phenotypic differences in T cell infiltration within the TME can be categorized into three types: the “immune-inflamed” phenotype, in which $CD8^+$ T cells infiltrate the tumor; the “immune-excluded” phenotype, in which infiltrating $CD8^+$ T cells accumulate in the tumor stroma and the “immune-desert” phenotype, in which $CD8^+$ T cells are low or absent from the

tumor and stroma (11). Recently, Ana et al (12) confirmed that commensal *Clostridiales* strains could enhance the immunity and transform the TME from “immune-desert” phenotype to “immune-inflamed” phenotype by increasing the frequencies and activity of tumor-infiltrating IFN-γ^+ $CD8^+$ T cells, which finally elevated the colorectal cancer patients’ prognosis. In this context, it has been shown that the efficacy of cancer therapies depends on the composition of the microbiome (13).

In gastric cancer, there is no consensus regarding the foe or friend role of the *H. pylori* infection in patients’ prognosis. Georgios et al (14) have reported that infection with *H. pylori* is associated with higher relapse-free survival and overall survival in patients who have curative resection without residual, local, or metastasised tumor. They speculated that cancer immunity might be suppressed in patients who are negative for *H. pylori*, conversely, both innate and adaptive immunity has been boosted sharply due to the *H. pylori* infection. However, the detailed mechanism still remained unknown. Here, we aim to identify whether *H. pylori* infection is contributing to the “immune-inflamed” TME, what is component of immune cells build up such TME and how did the differential immune cells influence the prognosis of gastric cancer patients. After prognosis analysis of gastric cancer in Chinese population, we isolated intratumoral $CD45^+$ immune cells in human gastric cancer tissues with or without *H. pylori* infection and addressed these questions by analysing *H. pylori*-specific immune cells of single cell sequencing. Our work promotes the understanding of heterogeneity between patients with different *H. pylori* infection status and provide a basis for individualized treatment for gastric cancer.

Methods

Study Population

Han ethnic Chinese patients with gastric cancer were recruited from the First Affiliated Hospital of Nanjing Medical University, the Northern Jiangsu People's Hospital and the Affiliated Hospital of Yangzhou University between 2006 and 2016. All of the cases were newly diagnosed, and had no treatment prior to recruitment including radiotherapy or chemotherapy. All case patients were histopathologically or cytologically confirmed to have gastric cancer by at least two local pathologists. After signing informed consent, we collected 5 mL of venous blood from the patients and conducted a face-to-face interview concerning demographic data (e.g., age and sex) and life style information (e.g., smoking and drinking) at recruitment. Furthermore, we reviewed patients' medical record to gather more detailed clinical information such as date of diagnosis, surgery status, histopathological type, clinical stage, and treatment. Patients with curative resection and non-cardia adenocarcinomas were included in the study. All patients’ survival time were acquired by personal or family contacts from the time of enrollment until death or last time of follow-up (last follow-up: June 2019) every 6 months. The follow-up data included treatment information (chemotherapy or radiotherapy) and survival status (alive or dead, time of death, and cause of death) and the latest medical records from their treating physicians were also checked as a complement. Finally, a total of 488 patients who had both available follow-up and clinical information were enrolled in this study.

Serology assay for *Helicobacter pylori* (*H. pylori*) infection

H. pylori infection status was determined using an *H. pylori* IgG ELISA kit (IBL International, Hamburg, Germany) according to the manufacturer’s instructions. Briefly, plasma *H. pylori* IgG antibody was measured using 5 μL plasma and each sample was quantified using a calibration curve. Positivity was determined when the *H. pylori* IgG antibody titer of a sample was >10 U/ml. Individuals were regarded negative for *H. pylori* if they had no history of *H. pylori* infection on questioning and if they were also negative in the *H. pylori* IgG ELISA test. Sensitivity and specificity for the *H. pylori* IgG ELISA, as provided by the manufacturer, were 96.0% and 96.0%, respectively.

Reagents and antibodies

The following anti-human fluorophore-conjugated antibodies were used for flow cytometry: CD45-BV510 (clone: HI30, cat. no. 304036, supplier: BioLegend), CD3-FITC (HIT3a, 300312, BioLegend), CD4-BV605 (RPA-T4, 562658, BD Biosciences), CD8-PerCP/Cy5.5 (SK1, 565310, BD Biosciences), CD45RA-FITC (HI100, 304106, BioLegend), CCR7-PE/Cyanine7 (G043H7, 353226, BioLegend). The following anti-human primary antibodies were used for multiplexed immunofluorescence staining CXCL13 (cat. No. ab272874, supplier: abcam), CD103 (ab224202, abcam), CD8 (ab237709, abcam), PTGER2 (ab124419, abcam) and AREG (sc-74501, SANTA CRUZ).

Isolation of TILs from gastric cancer biopsies

Following tumor excision or biopsy, a representative tumor fragment that was fresh and sterile was transferred to the laboratory for study. All surrounding macroscopic tissue, including any obvious tumor capsule, was removed from the tumor. Every sample was cut into small pieces (<1 mm in diameter) and then was incubated with RPMI 1640 containing 10% FBS, 1.5 mg ml-1 collagenase IV (LS004188, Worthington) and 0.5 mg ml-1 DNAse I (DN25-1G, Sigma) for 30 min on a 37 °C shaker (220 r.p.m). Digested tumor pieces were teased through a 70-μm strainer and diluted. After centrifugation, the cell pellet was resuspended in a 40% Percoll solution (170891, GE Healthcare), and a phase of 80% Percoll was underlaid using a glass Pasteur pipette. The resulting gradient was centrifuged at 2000 r.p.m for 30 min at room temperature without brakes. After removal of the red blood cell-containing pellet on the bottom and excess buffer-containing cellular debris on the top, the cell population at the Percoll interphase enriched for TILs was washed twice.

Antibody labeling cells for FACS

Homogenized cells were labeled with monoclonal antibodies for 30 min at 4 °C in FACS buffer (2% FBS in Dulbecco's PBS), washed twice in FACS buffer, then fixed IC Fixation buffer (00-8222-49, Invitrogen) in Dulbecco's PBS. Panel included CD45 to discriminate TILs from other cells in the cell suspension, T cell markers CD3, CD4 and CD8 and the T cell differentiation markers CD62L and CCR7. Viable cells were revealed using the Zombie NIRTM Fixable Viability Dye (BioLegend). Multiparameter FACS data was acquired on the BD LSR Fortessa X-20 FACS instrument (BD Biosciences), and data was analyzed using FlowJo software (version 10, Treestar Inc.).

Single-cell RNA sequencing of TILs

TILs of gastric cancer tissues were isolated as outlined above. The single-cell suspensions and the viable cells were FACS-sorted for CD3+CD45+ T cells on a BD FACSAria II Cell Sorter (BD Biosciences). The sorted cells were then resuspended at a 1×10^5-2×10^5 cells/ml concentration with a final viability of >80% as determined. Next, 4,000 cells per sample were targeted for scRNAseq on a Chromium Single Cell System (10× Genomics). Samples were processed as per the manufacturer's instructions (chromium single-cell 3'reagents, v3 chemistry), and libraries were sequenced on an Illumina NextSeq sequencer.

Pre-processing of sequencing results to generate transcript matrices was performed using the 10× Genomics Cell Ranger pipeline with default settings (v3.0.1). Further downstream analysis was performed in R using the Seurat package (v3.0.2). Cells were excluded if fewer than 200 or more than 5,000 genes were detected or if mitochondrial transcripts accounted for more than 40% of reads. Data were scaled and principal component analysis was performed using Seurat's default settings. Cells were clustered using the FindNeighbors (20 dimensions of reduction) and FindClusters functions at default settings; t-distributed stochastic neighbor embedding (tSNE) were calculated for visualizing clusters.

Differential gene expression analysis between each cluster was performed using the FindAllMarkers function in the Seurat package to the normalized gene expression data and each T cell sub-cluster was annotated according to DEGs. GO and KEGG enrichment analysis were performed on these DEGs with clusterProfiler package(15), while GSEA was also performed using a Python implementation (package gseapy) with the genesets of C5 and C7 in the MSigDB database (16).

To depict the developmental trajectory of $CD8^+$ T cells, the Monocle2 R (17) package was applied to the expression profiles of the cell subtypes. Briefly, the expression profiles (Seurat objects) were converted to Monocle cell data sets by the 'importCDS' function. Variably expressed genes selected by Seurat that had a mean expression between 0.125 and 3 and quantile-normalized variance larger than 0.5 were used as inputs. Putative trajectories were plotted using the 'plot_cell_trajectory' function after dimension reduction and cell ordering. To assess the functional states of $CD8^+$ T cells, several cytotoxicity-associated genes (NKG7, PRF1, GZMA, GZMB, GZMK, IFNG, CCL4 and CST7) and exhaustion associated genes (LAG3, TIGIT, PDCD1, HAVCR2 and CTLA4) were used to calculate the cytotoxicity score and exhaustion score.

Analyzing selected ligand-receptor pairs between $CD8^+$ T cells and epithelial cells

Single-cell RNA sequencing data of stomach tissues was downloaded from the GEO (GSE134520) (18). For a pair of investigated cell types, the level of interaction was analyzed by CellPhoneDB 2 (19), a Python-based computational analysis tool enables analysis of cell-cell communication at the molecular level, and defined as the product of the average expression levels of ligands in $CD8^+$ T cells and the average expression levels of their corresponding receptors in epithelial cells. To acquire the significance of a particular interaction, we conducted a permutation test by randomly shuffling the dataset of all cells 1000 times and generating a background distribution of interaction levels, based on which we calculated a *P*-value.

Multiplexed immunofluorescence staining

Multiple staining of tissues was performed using the PANO 4-plex immunohistochemistry kit (Cat# 10079100100, Panovue) according to manufacturer's instructions. In brief, we incubated paraffin slices with different primary antibodies (CXCL13, CD103, CD8 or PTGER2, CD8, AREG) after microwave heat treatment, then incubated them with horseradish peroxidase (HRP) conjugated secondary antibodies and amimide signal amplification. The slides were microwave heat treated again for another primary antibody incubation. DAPI staining was performed after all the antigens above had been labeled. Multi-spectral images were obtained by scanning stained slides using Mantra System (PerkinElmer), which captures fluorescence spectra at 20-nm wavelength intervals of 420 to 720 nm, with the same exposure time. On the basis of full film scanning, 5 high magnification fields were randomly selected from each tissue point for image capture. The selected field were scanned to obtain multi-spectral images using Mantra System, which captured fluorescence spectra at 20-nm wavelength intervals of 420-720 nm with the same exposure time.

Survival analyses

We performed univariate and multivariate analyses using the Cox proportional hazards model to correct clinical covariates including age, gender, smoking, drinking, clinical stage, chemotheraphy status, radiotheraphy status and *H. pylori* infection status for all survival analyses in our study. Kaplan-Meier survival curves were plotted to show differences

in survival time, and *P* values reported by the Cox regression models implemented in the R package survival were used to determine the statistical significance.

The gastric cancer data were used to evaluate the prognostic effect of individual genes or gene sets derived from specific cell clusters. We downloaded the gene expression data as well as clinical and follow-up data for patients with stomach adenocarcinoma (STAD) in the TCGA from the FireBrowse (http://firebrowse.org/) and other public gastric cancer datasets from the GEO (GSE84437, GSE62254 and GSE15459). The expression profile was normalized by z-scores of log2 (FPKM+1) to exclude potential bias. For individual genes, the relative gastric cancer patients were divided into high 50% and low 50% based on the median expression. Kaplan-Meier analysis was performed to evaluate the prognostic value of cell genes and detect the role that these genes play in gastric cancer progression.

In order to assess the prognostic value of the specific signature identified in the present study, the fold-change value for each gene in the CD8-C0-CXCL13 cluster was used to weight its expression level in the TCGA or GEO database, and Kaplan-Meier survival curves were generated by partitioning gastric cancer cases from the TCGA or GEO databases in two splits based on the median value of the weighted average expression of 27 DEGs which were identified in the CD8-C0-CXCL13 cluster as compared with the other clusters (p.adj $\leq$ 0.001 and log2FoldChange $\geq$ 0.5). For the univariable forest plots, hazard ratios were derived using Cox proportional hazards survival models in gastric cancer cases with the overall survival.

Correlation analysis between genes and the level of immune infiltration of gastric cancer

The TIMER2.0 (20) is a friendly platform for systematical evaluations of the clinical impact of different immune cells in diverse cancer types. “Immune estimation module” refers to analyzing immune infiltration estimations for users-provided expression profiles by TIMER, CIBERSORT, quanTIseq, xCell, MCP-counter and EPIC algorithms. We have studied whether the expression of *TNFRSF1A* or *DAG1* gene is related to the level of immune infiltration in STAD. The correlations between *TNFRSF1A* or *DAG1* gene expression and $CD8^+$ T cell, $CD8^+$ TEM cell and $CD8^+$ naive cell were analyzed.

Statistical analysis

All statistical analyses and graph generation were performed in R (version 4.0.3). Groups were compared using tests for significance as indicated in the figure legends and the text. A significant difference was concluded at $P<0.05$.

Results

H. pylori infection was associated with better survival in Chinese gastric cancer patients

In order to test the infection of *H. pylori* on the survival of gastric cancer, a total of 488 patients were enrolled in the study and divided into two groups according to the *H. pylori* infection status (Supplementary Table 1). Among these patients, 372 men and 116 women participated with median age of 63 years, in which 224 were negative for *H. pylori* (hereafter “*H. pylori* -”) whereas the rest of the participants□264 patients□were *H. pylori* positive (hereafter “*H. pylori* +”). The *H. pylori* positive rate was 54.10%, which was consistent with the overall *H. pylori* infection rate in Chinese population with 55.8% (21). In addition, there were more smokers and drinkers in the *H. pylori* + group, while the patients with stage IV was relative lower than the *H. pylori* - group. For the chemotherapy after surgical operation, 67.41% patients in the *H. pylori* - group accepted the chemotherapy, higher than those in the *H. pylori* + group (58.33%).

As shown in Table 1, the median survival time was 36.33 months, and 190 patients (38.93%) died of gastric cancer in our cohort. The median survival time was 142.3 months in patients positive for *H. pylori*, compared with 82.1 months in patients negative for *H. pylori* (Figure 1A, HR=0.64, 95% CI=0.48-0.85, P=2.35×10^{-3}). In addition, we found that age, gender, clinical stage, and radiotherapy were significantly associated with the survival of our subjects with gastric cancer (Table 1, Figure1B and Supplementary Figure 1). In multivariate analyses, we revealed that positive *H. pylori* status was significantly associated with better prognosis of gastric cancer, with adjustments of age, gender, clinical stage and radiotherapy status. Additionally, age and gender were also prognostic factors for overall survival (Table 1). When adjusted for all variables in our study, only clinical stage and *H. pylori* status were independent prognostic factor for survival, in which patients with positive *H. pylori* status had a significantly longer survival time compared to patients with negative *H. pylori* status (Table 1, HR=0.74, 95% CI=0.55-0.99, P= 0.045).

Table 1

Univariate and multivariate analysis of predictive factors for overall survival in 488 patients with gastric cancer

Variables	Patients	Deaths	MST (mo)	HR (95% CI)	*P*	Adjusted HR (95% CI) [a]	Adjusted *P*[a]	Adjusted HR (95% CI) [b]	Adjusted *P*[b]
	N=488	N=190							
Age									
< 63	244	83	133.3	1.00		1.00		1.00	
≥ 63	244	107	84.3	1.44 (1.08-1.92)	**0.012**	1.39 (1.04-1.86)	**0.025**	1.32 (0.98-1.78)	0.070
Gender									
Male	372	157	85.2	1.00		1.00		1.00	
Female	116	33	NA	0.64 (0.44-0.93)	**0.018**	0.68 (0.46-0.99)	**0.044**	0.64 (0.43-0.95)	**0.026**
Smoker									
No	324	123	101.3	1.00		1.00		1.00	
Yes	164	67	83.4	1.01 (0.75-1.36)	0.946	0.95 (0.70-1.31)	0.771	1.02 (0.68-1.54)	0.921
Drinker									
No	351	132	101.3	1.00		1.00		1.00	
Yes	137	58	83.4	1.02 (0.75-1.39)	0.905	0.89 (0.64-1.22)	0.458	0.88 (0.58-1.33)	0.536
Clinical stage									
AJCC I	102	10	NA	1.00		1.00		1.00	
AJCC II	71	21	142.3	2.69 (1.26-5.73)	**0.010**	2.52 (1.18-5.37)	**0.017**	2.61 (1.22-5.59)	**0.013**
AJCC III	137	63	83.4	5.19 (2.66-10.11)	**1.37×10^{-6}**	4.72 (2.41-9.24)	**6.00×10^{-6}**	4.92 (2.50-9.66)	**3.77×10^{-6}**
AJCC IV	178	96	30.2	13.77 (7.07-26.82)	**1.27×10^{-14}**	11.94 (6.09-23.40)	**1.27×10^{-14}**	12.56 (6.39-24.70)	**2.25×10^{-13}**
P trend				2.37 (1.98-2.84)	**$< 2.0\times10^{-16}$**	2.27 (1.89-2.72)	**$< 2.0\times10^{-16}$**	2.29 (1.91-2.76)	**$< 2.0\times10^{-16}$**
Chemotherapy									
No	183	65	NA	1.00		1.00		1.00	
Yes	305	125	88.0	1.06 (0.78-1.43)	0.713	0.81 (0.58-1.12)	0.200	0.81 (0.58-1.13)	0.212
Radiotherapy									

No	429	158	133.3	1.00		1.00		1.00	
Yes	59	32	63.7	1.73 (1.18-2.53)	**5.12×10^{-3}**	1.32 (0.90-1.95)	0.158	1.41 (0.94-2.12)	0.096
H. pylori									
Negative	224	100	82.1	1.00		1.00		1.00	
Positive	264	90	142.3	0.64 (0.48-0.85)	**2.35×10^{-3}**	0.74 (0.56-1.00)	**0.049**	0.74 (0.55-0.99)	**0.045**

[a]Adjusted for age, gender, clinical stage, radiotheraphy status and *H. pylori* infection status.

[b]Adjusted for age, gender, smoking, drinking, clinical stage, chemotheraphy status, radiotheraphy status and *H. pylori* infection status.

H. pylori, *Helicobacter pylori*

Especially, for patients with early and intermediate stage gastric cancer (ie, AJCC I, II and III), we found a significant difference in overall survival between those who were positive for *H. pylori* and those who were negative (P=0.024); however, we found no such association for patients with advanced cancer (ie, AJCC IV, P=0.979, Figure 1C). Findings were much the same on stratification of patients by other classifications for early and intermediate versus advanced disease, like patients who were positive for *H. pylori* status had significantly higher survival than did those who were negative only for those with tumor depth without invasion of visceral peritoneum or adjacent structures (ie, T1, T2 and T3, P=0.028, Supplementary Figure 2A) and for those with nodal involvement less than 2 (ie, N0 and N1, $P=1.3\times10^{-3}$, Supplementary Figure 2B). Hence, we identified *H. pylori* as an independent, beneficial prognostic factor, the effect of which was most pronounced in patients with early-stage cancer.

H. pylori affect gastric cancer mainly targeting $CD8^+$ T cells within tumor microenvironment

It has been suggested that tumor-specific immune responses are upregulated in patients with gastric cancer who are positive for *H. pylori* (14). In order to evaluate the possible immune mechanism of *H. pylori* on gastric cancer microenvironment, we first explored the content of tumor-infiltrating lymphocytes (TILs) and found that $CD3^+$ T cells were the dominant TIL population both in *H. pylori* - and *H. pylori* + group (Supplementary Figure 3A). As $CD8^+$ T cells play a pivotal role in clearing intracellular pathogens and tumors (22), we next examined the frequency of naive and memory subsets of $CD3^+CD8^+$ T cells based on CD45RA and CCR7 expression. We found that the effector memory T cell (T_{EM}, $CD45RA^-CCR7^-$) followed by central memory T cell (T_{CM}, $CD45RA^-CCR7^+$) were the most prevalent subsets. In addition, the frequency of T_{EM} in *H. pylori* + gastric cancer was much more compared with *H. pylori* - gastric cancer (Supplementary Figure 3B), which indicated that *H. pylori* + gastric cancer have a stronger immediate effector function than *H. pylori* - gastric cancer.

Single-cell transcriptomic profiling of the T cells in gastric cancer tumors among different *H. pylori* infection status

To shed light on the complexity of tumor-infiltrating T cells in gastric cancer in an unbiased manner, we further conducted 3' droplet-based scRNA-seq (BD Rhapsody^{TM}) on 18,717 flow-sorted $CD3^+CD45^+$ T cells freshly isolated from 3 *H. pylori* - and 3 *H. pylori* + gastric cancer patients (Figure 2A and Supplementary Table 2). T cell clusters were visualized using t-distributed stochastic neighbor embedding (t-SNE) after preprocessing, normalization and batch correction (Supplementary Figure 4). Overall, we identified ten unique clusters based on their gene expression profiles, including six distinct $CD8^+$ T cell clusters and four distinct $CD4^+$ T cell clusters (Supplementary Figure 5A-C). Each of the ten clusters harbored differentially expressed genes (DEGs) representing distinct cell types or subtypes (Supplementary Table 3 and Supplementary Figure 5D).

To address the intrinsic T cell heterogeneity, we applied unsupervised re-clustering based on t-SNE and identified ten $CD4^+$ and twelve $CD8^+$ clusters (Figure 2B, Supplementary Figure 6). We further surveyed the expression and distribution of canonical T cell markers among these clusters, respectively (Figure 2C, Supplementary Figure 7). Among the ten $CD4^+$ T cell clusters (Supplementary Table 4), we found that CD4-C2-FOXP3, CD4-C3-TNFRSF4, CD4-C8-COL5A3 and CD4-C9-IFIT1 clusters represented regulatory T cells (Tregs) with high expression levels of *FOXP3*, *IKZF2* and *IL2RA*, as well as coinhibitory molecules *TIGIT* and *CTLA4* (Figure 2C, Supplementary Figure 7A). Cells in CD4-C5-CXCL13 and CD4-C6-TOX2 showed high expression levels of *PDCD1* and *CXCL13* (Figure 2C, Supplementary Figure 7A), thus representing follicular T helper cells involved in the formation of ectopic lymphoid-like structures in inflammatory sites (23). Two clusters of $CD4^+$ T cells (CD4-C1-CCR7 and CD4-C7-FBLN7) were characterized by a gene signature including *CCR7*, *LEF1*, *TCF7* and *SELL* (Figure 2C, Supplementary Figure 7A), which are typical features of naive T cells. Of interest, T cells from CD4-C0-CCL5 and CD4-C4-SLC4A10 showed high expression levels of *CD69*, which has recently been reported to be elevated in activating MAIT cells of patients with COVID-19 (24). Given that the MAIT cells can display effector functions involved in the defense against infectious pathogens (25). We found that the proportion of these two clusters were relatively increased in *H. pylori* + (Supplementary Figure 7B), which may be activated by *H. pylori*.

When focusing on the different $CD8A^+$ clusters (Supplementary Table 5), we noted that CD8-C7-KLF2 characterized by a gene signature including *CCR7*, *LEF1*, *TCF7* and *SELL*, which are typical features of naive T cells (Figure 2C, Supplementary Figure 7C). Among identified $CD8^+$ T_{EM}, which characterized by low expression of CCR7, CD8-C0-CXCL13, CD8-C5-XCL2, CD8-C8-HSPA1B and CD8-C10-IFIT1 T cells with an activated cellular state ($CD8^+$ T_{EM} activated-state), characterized by the expression of effector molecules such as *IFNG*, *CCL4* and *CCL5* (Figure 2C, Supplementary Figure 7C); and CD8-C6-FGFBP2 T cells, with features of natural killer (NK) cells, expressing genes such as *NKG7*, *FGFBP2*, and *FCGR3A*, which we refer to as '$CD8^+$ T_{EM} NK-like' (Figure 2C, Supplementary Figure 7C). Interestingly, CD8-C0-CXCL13 and CD8-C10-IFIT1 also exhibited variable expression of exhaustion markers, like *LAG3*, *HAVCR2* and *PDCD1* (Figure 2C, Supplementary Figure 7C), indicating an activation-coupled exhaustion program putatively caused by both *H. pylori* infection and tumor cells. Besides, cytotoxic $CD8^+$ T cells ($CD8^+$ $T_{CYTOTOXIC}$) from CD8-C1-ZNF683 and CD8-C9-KIR2DL3 showed high expression levels of cytotoxicity-related genes such as *GNLY*, *GZMB*, *PRF1* and tissue residency gene *ZNF683* (HOBIT) (Figure 2C, Supplementary Figure 7C). We further noted that CD8-C4-AREG cluster had expression of molecules suggestive of a tissue-resident memory T cells (T_{RM}) with high expression of *ITGAE* (*CD103*), *ITGA1* and *CD69*, while showing low expression of *SELL*, *S1PR1* and *KLF2* (Figure 2C, Supplementary Figure 7C), akin to T_{RM} cells described in humans and mice (26). CD8-C11-TRDC was assigned to T-gd cells, expressing *TRDC*, *TRGC1*, and genes associated with cytotoxicity, including *GNLY* (27), while CD8-C2-*KLRB1* cluster was characterized by high expression of *KLRB1*, which are known hallmarks of mucosal-associated invariant T cells (Figure 2C, Supplementary Figure 7C) (28).

Unlike $CD4^+$ T cells (Supplementary Figure 7B), the clusters in $CD8^+$ T cells appeared to exhibit distinct distributions. Especially, CD8-C0-CXCL13, contained mostly cells of *H. pylori* +, while CD8-C4-AREG and CD8-C7-KLF2 were almost exclusively populated with cells from *H. pylori* - (Supplementary Figure 7D). We further analyzed the developmental fate

of these differentially distributed cells using the Monocle 2 algorithm to establish a pseudotemporal ordering reflective of cell lineage. Since cluster CD8-C7-KLF2 was naive T cells, two major developmental trajectories were observed (Figure 2D), in which the T_{RM}-like and T_{EM} activated-state cells were located at opposite ends of the pseudotime path, supporting the distinct gene expression profiles of these cells. In addition, we also calculated a cytotoxicity score and exhaustion score for each cell based on the expression of canonical markers. Along the trajectory, most $CD8^+$ T cells exhibited gradually increasing cytotoxic activity, which was accompanied by gradually increasing exhaustion (Figure 2E). Especially, the score of cytotoxic activity was downregulated in trajectory 1 toward cluster CD8-C4-AREG cells, while was increased in trajectory 2 of both CD8-C0-CXCL13 and CD8-C10-IFIT1 T cells (Figure 2F), which retained the ability for active cell division in the immune microenvironment. Hence, we show using single-cell analysis that the $CD8^+$ population is heterogeneous with distinct subsets.

H. pylori infection promote intratumoral immune activation with enhanced interaction between $CD8^+$ T cells and epithelium

We first focusing on CD8-C0-CXCL13 cluster, we noted that except for the high expression of *CXCL13*, it also specifically expressed genes like *MYO7A*, *TOX* and *PHLDA1* (Figure 3A). We then compared the single cell data between CD8-C0-CXCL13 group and the other groups to determine the differential expression genes, 192 up-regulated and 118 down-regulated genes were detected in CD8-C0-CXCL13 T cells ($p.adj \leq 0.01$ and $|\log_2 FoldChange| \geq 0.25$) (Supplementary Figure 8A and Supplementary Table 6). Gene ontology (GO) functional enrichment analysis revealed that these upregulated genes in CD8-C0-CXCL13 T cells were enriched for signaling pathways such as T cell activation, regulation of lymphocyte activation and regulation of T cell activation (Supplementary Figure 8B). There are also other enriched gene sets that are crucial for anti-pathogen infection such as Th1 and Th2 cell differentiation, Th17 cell differentiation as well as antigen processing and presentation by KEGG analysis (Supplementary Figure 8C), which was potentially associated with *H. pylori* infection.

To further decipher the molecular characteristics difference of CD8-C0-CXCL13 T cells resulted from *H. pylori*, gene set enrichment analysis (GSEA) was conducted and we revealed that T cells from *H. pylori* + were associated with cell activation involved in immune response and regulation of response to cytokine stimulus, indicating a potential protection role against local *H. pylori* infections (Figure 3B). In addition, we investigated the expression level of genes between *H. pylori* infection status. Interestingly, we found that cytotoxicity-associated genes, such as *IFNG* and *GZMB* were upregulated in the patients with *H. pylori* +, while the expression of exhaustion marker *PDCD1* was downregulated (Figure 3C). As expected, a higher level of *IFNG* and *GZMB* were associated with a better prognosis in gastric cancer (Supplementary Figure 8D, 8E).

Early studies established the concept that gastric epithelial cells from *H. pylori* infected patients contain increased TNF receptors against invading infection with subsequent activation of an adaptive immune response. Using data from single cell sequencing of stomach tissues (GSE134520), we estimated TNF-dependent T cell functions in $CD8^+$ T cells and epithelium. We found prominent TNF-TNFRSF1A and TNF-DAG1 interaction in stomach, which was enhanced with *H. pylori* infection (Figure 3D), suggesting that the molecular interaction is crucial in creating an immune activation tumor microenvironment with the response to *H. pylori* infection. Notably, *TNFRSF1A*, not *DAG1*, was positively correlated with the $CD8^+$ T cells signature as well as T_{EM} signature, while negatively correlated with the naïve T cells in the TCGA STAD cohort using the TIMER2.0 webserver (Supplementary Figure 8F), which indicated that *TNFRSF1A* may play an important role to induce antitumor immunity against gastric cancer. More important, using bulk RNA sequencing data from normal gastric mucosa tissues, we found that the expression of *TNFRSF1A* was significantly increased in samples with *H. pylori*

infection, while *DAG1* was not changed (Figure 3E). Together, our results predicted that *H. pylori* infection potentially be able to recruit T cells into the tumor by *TNFRSF1A-TNF* interaction and then enhanced the immune activity.

As our data suggest that the CD8-C0-CXCL13 T cell subset is a highly prevalent effector population in the microenvironment of gastric cancer, we predicted that the single-cell-derived gene signature from the CD8-C0-CXCL13 cluster (Supplementary Table 5) would provide important prognostic information. Using available gene expression data, we found that the CD8-C0-CXCL13 signature was significantly associated with improved overall survival (Figure 4A). We further performed multicolor immunofluorescence staining on stroma and tumor sections from gastric cancer patients. Among $CD8^+$ T cells, *CXCL13* and CD103 were both activated by *H. pylori* infection in stroma and tumor tissues (Figure 4B), supporting the presence of these activated cells in gastric cancer.

T_{RM} cells marked by PTGER2 worsen prognosis in *H. pylori* negative gastric cancer

It has been reported that there exists virus- or other pathogen-specific (bystander) $CD8^+$ T_{RM}-like cells in tumor and can be re-activated to induce antitumor immunity (29). However, we found 151 down-regulated genes in CD8-C4-AREG T cells ($p.adj \leq 0.01$ and $|\log_2 FoldChange| \geq 0.25$) (Supplementary Figure 9A and Supplementary Table 7), enriched for signaling pathways such as T cell activation, response to IFN-γ and antigen processing and presentation (Supplementary Figure 9B), which indicated an immunosuppression state in CD8-C4-AREG T_{RM} cells. In addition, though we found that the gene expression profiles of these T cells were similar between *H. pylori* - and *H. pylori* + (Figure 5A), GSEA analysis revealed that T cells from *H. pylori* + were associated with inflammatory response and cytokine mediated signaling pathway (Figure 5B, Supplementary Figure 9C), while response to steroid hormone pathway was enriched in T cells from *H. pylori* – (Supplementary Figure 9C), in which *AREG* and *PTGER2* were both increased (Figure 5C). Similarly, further immunohistochemistry staining also confirmed that *AREG* and *PTGER2* were both inactivated by *H. pylori* infection in stroma and tumor tissues (Figure 5D). Using prognostic data from TCGA and GSE15459, we show that the *PTGER2* can discriminate between patients with high CD8 expression, in which high *PTGER2* expression was significantly associated with worse prognosis, but not in patients with low CD8 expression (Figure 5E and Supplementary Figure 9D). These data suggest that T_{RM} cells with high expression of *PTGER2* may be the key therapeutic target to improve the clinical outcomes of gastric cancer.

Discussion

On the one hand, we conducted prognosis analysis of gastric cancer patients with different *H. pylori* infection status from the population level. On the other hand, a single-cell transcriptome profiling from molecular level was performed which allowed for the characterization of different T cell subpopulations and *H. pylori* activated clusters, as well as for the delineation of transcriptional changes in *H. pylori* activated T cells, and the identification of co-stimulatory ligand expression in *H. pylori* + gastric cancer cells. The results of this study shed light into the mechanisms underlying the target cell dependent T cell responses induced by *H. pylori*, as well as the potential mechanisms underlying the responses of gastric cancer patients to *H. pylori* infection and indicate that *PTGER2* may serve as a potential target to treat patients with gastric cancer.

Though it is well established that *H. pylori* infection contributes greatly to the carcinogenesis of gastric cancer, the role of *H. pylori* infection in predicting the gastric cancer patients' survival is still less well understood. Interestingly, a prospective study has demonstrated that gastric cancer patients with positive *H. pylori* infection frequently showed better relapse-free survival and better overall survival (14). In addition, other studies (30, 31), especially a meta-analysis demonstrated that *H. pylori* infection is an independent protective factor for gastric cancer progression, in which this

protective effect is stable among different ethnic groups, different *H. pylori* evaluation methods and quality assessment measures (32). Similar to these results, our study also confirmed that *H. pylori* is an independent, beneficial prognostic factor, especially in patients with early-stage gastric cancer. This may be attributed to *H. pylori* infection not being the only factor affecting the prognosis and many types of therapies being available for advanced or relapsed gastric cancer patients (33).

The suppressive effect of *H. pylori* on gastric cancer progression is possibly due to the induction of some antitumor immunity. It has been shown that the activation of T cells, the main immune effector cells for acquired immunity, are directly affected by *H. pylori* bacterial products, e.g., VacA and arginase (34, 35). Besides, several naturally occurring immunodominant $CD4^+$ T cell responses in *H. pylori*-infected subjects has also been identified and characterized (36). In here, though we didn't see significant difference between $CD4^+$ T cells, we identified two clusters exhibit distinct distributions in $CD8^+$ T cells among different *H. pylori* infection status. Since the immunodominant T cells are believed to be more effective and play a central role in the host adaptive immunity against pathogens which has been well demonstrated in many viral, bacterial, and tumor systems (37, 38). Previous researches have shown increased gastric T-cell infiltration in situ with a typical T-helper (Th)1 phenotype during *H. pylori* infection (39) and identified several antigen-specific T-cell response like HpaA-specific mucosal $CD4^+$ T-cell responses with a Th1 profile, which occurred mainly in the period of precancerous lesions (36). However, in cancer, including gastric cancer, $CD8^+$ T cells are essential for immune defence to eradicate cancer cells though always become dysfunctional over the course of tumorigenesis (40). In order to solve this problem, researchers have developed a series of immunotherapy, such as immune checkpoint blockade (41), adoptive T cell therapy (42), chimeric antigen receptor T cell therapy (43) and cancer vaccines (44), to restore the functions of $CD8^+$ T cells. Hence, we have reason to speculate that these specific $CD8^+$ T cells driven by *H. pylori* may be the reason for the better prognosis of gastric cancer patients with *H. pylori* infection.

Recent technological advances have provided important insights into the heterogeneity of $CD8^+$ TILs, demonstrating that distinct T cell subsets exist with different transcriptional programmes and functional states (40). When focusing on CD8-C0-CXCL13 cluster, we noted that except for the high expression of *CXCL13*, it also specifically expressed genes like *TOX*, a key transcription factor for $CD8^+$ T cell differentiation during chronic viral infections and cancer (45) and *PHLDA1*, a required transcription factor for regulation of the TLR-mediated immune response (46), reflecting these cells has a strong immunological activity state. Consistent with the characteristic, pathway enrichment analysis revealed that these upregulated genes in CD8-C0-CXCL13 T cells were enriched with T cell activation.

Since the epithelial cells are at the center of the cellular interaction network in gastric cancer, defining the molecular characteristics of tumor tissues (47). We investigated and evaluated the interaction between epithelial cells and matched $CD8^+$ T cells. The data suggest that tumor cells with strong *TNFRSF1A* expression might directly interact with *TNF* of $CD8^+$ T cells and enhance $CD8^+$ T cell activity by producing *GZMB* and *IFNG*, suppressing tumor progression in gastric cancer with *H. pylori*. More importantly, as the single-cell-derived gene signature could provide prognostic information, a series of immune cell signatures were identified by single cell sequencing in such as breast cancer (48), lung cancer (49) and melanoma (50), which were associated with patients' prognosis. Similarity, we confirmed that CD8-C0-CXCL13 T cells may be the key mediator of the improved clinical outcomes observed in human gastric cancer with *H. pylori* infection.

Recently, T_{RM} cells have been shown to both prevent and exacerbate pathologies (51). The involvement of T_{RM} cells in a range of human diseases makes the design of therapeutic strategies that can modulate either their production or their activity an attractive goal. In addition, more and more researches have confirmed that T_{RM} cells display transcriptional features that are specific to individual tissues and allow their survival and long-term retention at those different sites (52). Here, we identified a T_{RM} cell cluster marked by *AREG*, a member of epidermal growth factor family and *PTGER2*, a

receptor for prostaglandin E2, were almost exclusively populated with cells from *H. pylori* -. *AREG* has been shown to associate with type 2 immune-mediated resistance and tolerance mechanisms to infection, as well as promote immune suppression in the TME (53), while *PTGER2* enhanced the pathogenic phenotype by regulating the cytokines balance such as IFN-γ/IL-10 in a context dependent manner (54). More importantly, previous researches have revealed that *PTGER2* was overexpressed in many cancers and promotes tumor cell proliferation, invasion and prognosis (55). Here, we found that high *PTGER2* expression was significantly associated with worse prognosis only in patients with high CD8 expression of gastric cancer, just like one research confirmed that $CD8^+CD103^+$ T_{RM} cell subset was significantly associated with improved relapse-free and overall survival in triple negative breast cancers (48), which suggesting that T_{RM} cells with high expression of *PTGER2* may be a promising new prognostic factor and target for anti-cancer therapies.

There are several limitations of the present study. First, to investigate the effect of *H. pylori* on the survival of patients with gastric cancer, we chose a longitudinal study design. However, because our data are from one center, the results need to be validated further. Second, we focused on TILs in gastric cancer and performed scRNA-seq of T cells, the ligand-receptor interactions was inferred from public database mainly consist of normal tissues, further scRNA-seq data integrated of the tumor cells and TME cells from gastric cancer patients, as well as functional assays, will be more convincing. Third, due to a lack of immune competent animal model for gastric cancer, the direct or indirect mechanisms whereby this would occur *in vivo* are unclear.

In summary, we applied single-cell RNA sequencing to gastric cancer patients and characterized their T cell landscape with high resolution between different *H. pylori* infection status. We identified two $CD8^+$ T cell clusters, one cluster of $CD8^+$ T_{EM} activated-state cells, probably preceding activation by *H. pylori*, predicting better prognosis in gastric cancer, while one cluster of T_{RM} cells which almost exclusively populated with cells from *H. pylori* -, probably preceding exhaustion and predicting worse prognosis in gastric cancer. Our findings provide valuable resources for deciphering gene expression landscapes of heterogeneous cell types in gastric cancer and deep insight into cancer immunology for drug discovery in the future.

Declarations

Ethics approval and consent to participate:

The study was performed in accordance with guidelines outlined in the Declaration of Helsinki and approved by the institutional review board of Nanjing Medical University (FWA00001501). All study participants provided written informed consent.

Consent for publication:

Not applicable

Availability of data and materials:

The data generated in this study are not publicly available due to information that could compromise patient privacy or consent but are available upon reasonable request from the corresponding author.

Competing interests:

The authors have declared that no conflict of interest exists

Funding:

This work was supported by grants from the National Natural Science Foundation of China (82071767, 82125033, 82003534, 81872702, 81772978 and 81972626), the Natural Science Foundation of Jiangsu Province (BK20200674) and the Key Research and Development Program of Jiangsu Province (BE2019698). The funders had no role in the study design, data collection, data analysis, interpretation of data, or preparation of the manuscript.

Author Contributions:

Y.C., R.J. and Y.D. designed the study and edited the manuscript; C.Y. and S.S. performed statistical analysis and wrote the manuscript; C.Z. and D.K. performed the experiments; C.R., L.B., Y.G., Q.S. and B.D. participated in sample collection; J.C. contributed to discussion and reviewed the manuscript; Y.C. had primary responsibility for final content.

Acknowledgements:

Not applicable

References

1. Schistosomes, liver flukes and Helicobacter pylori. IARC Working Group on the Evaluation of Carcinogenic Risks to Humans. Lyon, 7-14 June 1994. IARC Monogr Eval Carcinog Risks Hum. 1994;61:1-241.
2. Malfertheiner P, Megraud F, O'Morain CA, Gisbert JP, Kuipers EJ, Axon AT, et al. Management of Helicobacter pylori infection-the Maastricht V/Florence Consensus Report. Gut. 2017;66(1):6-30.
3. Hatakeyama M. Helicobacter pylori CagA and gastric cancer: a paradigm for hit-and-run carcinogenesis. Cell Host Microbe. 2014;15(3):306-16.
4. Correa P, Fontham ET, Bravo JC, Bravo LE, Ruiz B, Zarama G, et al. Chemoprevention of gastric dysplasia: randomized trial of antioxidant supplements and anti-helicobacter pylori therapy. J Natl Cancer Inst. 2000;92(23):1881-8.
5. Wong BC, Zhang L, Ma JL, Pan KF, Li JY, Shen L, et al. Effects of selective COX-2 inhibitor and Helicobacter pylori eradication on precancerous gastric lesions. Gut. 2012;61(6):812-8.
6. Sheh A, Fox JG. The role of the gastrointestinal microbiome in Helicobacter pylori pathogenesis. Gut Microbes. 2013;4(6):505-31.
7. Amieva M, Peek RM, Jr. Pathobiology of Helicobacter pylori-Induced Gastric Cancer. Gastroenterology. 2016;150(1):64-78.
8. Roviello G, Iannone LF, Bersanelli M, Mini E, Catalano M. The gut microbiome and efficacy of cancer immunotherapy. Pharmacol Ther. 2021:107973.
9. Beura LK, Hamilton SE, Bi K, Schenkel JM, Odumade OA, Casey KA, et al. Normalizing the environment recapitulates adult human immune traits in laboratory mice. Nature. 2016;532(7600):512-6.
10. Sethi V, Vitiello GA, Saxena D, Miller G, Dudeja V. The Role of the Microbiome in Immunologic Development and its Implication For Pancreatic Cancer Immunotherapy. Gastroenterology. 2019;156(7):2097-115.e2.
11. Binnewies M, Roberts EW, Kersten K, Chan V, Fearon DF, Merad M, et al. Understanding the tumor immune microenvironment (TIME) for effective therapy. Nat Med. 2018;24(5):541-50.

12. Montalban-Arques A, Katkeviciute E, Busenhart P, Bircher A, Wirbel J, Zeller G, et al. Commensal Clostridiales strains mediate effective anti-cancer immune response against solid tumors. Cell Host Microbe. 2021;29(10):1573-88.e7.
13. Vétizou M, Pitt JM, Daillère R, Lepage P, Waldschmitt N, Flament C, et al. Anticancer immunotherapy by CTLA-4 blockade relies on the gut microbiota. Science. 2015;350(6264):1079-84.
14. Meimarakis G, Winter H, Assmann I, Kopp R, Lehn N, Kist M, et al. Helicobacter pylori as a prognostic indicator after curative resection of gastric carcinoma: a prospective study. Lancet Oncol. 2006;7(3):211-22.
15. Yu G, Wang LG, Han Y, He QY. clusterProfiler: an R package for comparing biological themes among gene clusters. OMICS. 2012;16(5):284-7.
16. Subramanian A, Tamayo P, Mootha VK, Mukherjee S, Ebert BL, Gillette MA, et al. Gene set enrichment analysis: a knowledge-based approach for interpreting genome-wide expression profiles. Proc Natl Acad Sci U S A. 2005;102(43):15545-50.
17. Qiu X, Mao Q, Tang Y, Wang L, Chawla R, Pliner HA, et al. Reversed graph embedding resolves complex single-cell trajectories. Nat Methods. 2017;14(10):979-82.
18. Zhang P, Yang M, Zhang Y, Xiao S, Lai X, Tan A, et al. Dissecting the Single-Cell Transcriptome Network Underlying Gastric Premalignant Lesions and Early Gastric Cancer. Cell Rep. 2019;27(6):1934-47.e5.
19. Efremova M, Vento-Tormo M, Teichmann SA, Vento-Tormo R. CellPhoneDB: inferring cell-cell communication from combined expression of multi-subunit ligand-receptor complexes. Nat Protoc. 2020;15(4):1484-506.
20. Li T, Fu J, Zeng Z, Cohen D, Li J, Chen Q, et al. TIMER2.0 for analysis of tumor-infiltrating immune cells. Nucleic Acids Res. 2020;48(W1):W509-w14.
21. Hooi JKY, Lai WY, Ng WK, Suen MMY, Underwood FE, Tanyingoh D, et al. Global Prevalence of Helicobacter pylori Infection: Systematic Review and Meta-Analysis. Gastroenterology. 2017;153(2):420-9.
22. Kaech SM, Cui W. Transcriptional control of effector and memory CD8+ T cell differentiation. Nat Rev Immunol. 2012;12(11):749-61.
23. Weichselbaum RR, Ishwaran H, Yoon T, Nuyten DS, Baker SW, Khodarev N, et al. An interferon-related gene signature for DNA damage resistance is a predictive marker for chemotherapy and radiation for breast cancer. Proc Natl Acad Sci U S A. 2008;105(47):18490-5.
24. Flament H, Rouland M, Beaudoin L, Toubal A, Bertrand L, Lebourgeois S, et al. Outcome of SARS-CoV-2 infection is linked to MAIT cell activation and cytotoxicity. Nat Immunol. 2021;22(3):322-35.
25. Legoux F, Salou M, Lantz O. MAIT Cell Development and Functions: the Microbial Connection. Immunity. 2020;53(4):710-23.
26. Kumar BV, Ma W, Miron M, Granot T, Guyer RS, Carpenter DJ, et al. Human Tissue-Resident Memory T Cells Are Defined by Core Transcriptional and Functional Signatures in Lymphoid and Mucosal Sites. Cell Rep. 2017;20(12):2921-34.
27. Poch T, Krause J, Casar C, Liwinski T, Glau L, Kaufmann M, et al. Single-cell atlas of hepatic T cells reveals expansion of liver-resident naive-like CD4(+) T cells in primary sclerosing cholangitis. J Hepatol. 2021;75(2):414-23.
28. Walker LJ, Kang YH, Smith MO, Tharmalingham H, Ramamurthy N, Fleming VM, et al. Human MAIT and CD8αα cells develop from a pool of type-17 precommitted CD8+ T cells. Blood. 2012;119(2):422-33.
29. Wang T, Shen Y, Luyten S, Yang Y, Jiang X. Tissue-resident memory CD8(+) T cells in cancer immunology and immunotherapy. Pharmacol Res. 2020;159:104876.
30. Kang SY, Han JH, Ahn MS, Lee HW, Jeong SH, Park JS, et al. Helicobacter pylori infection as an independent prognostic factor for locally advanced gastric cancer patients treated with adjuvant chemotherapy after curative resection. Int J Cancer. 2012;130(4):948-58.

31. Marrelli D, Pedrazzani C, Berardi A, Corso G, Neri A, Garosi L, et al. Negative Helicobacter pylori status is associated with poor prognosis in patients with gastric cancer. Cancer. 2009;115(10):2071-80.
32. Wang F, Sun G, Zou Y, Zhong F, Ma T, Li X. Protective role of Helicobacter pylori infection in prognosis of gastric cancer: evidence from 2,454 patients with gastric cancer. PLoS ONE. 2013;8(5):e62440.
33. Joshi SS, Badgwell BD. Current treatment and recent progress in gastric cancer. CA Cancer J Clin. 2021;71(3):264-79.
34. Karkhah A, Ebrahimpour S, Rostamtabar M, Koppolu V, Darvish S, Vasigala VKR, et al. Helicobacter pylori evasion strategies of the host innate and adaptive immune responses to survive and develop gastrointestinal diseases. Microbiol Res. 2019;218:49-57.
35. Chaturvedi R, de Sablet T, Coburn LA, Gobert AP, Wilson KT. Arginine and polyamines in Helicobacter pylori-induced immune dysregulation and gastric carcinogenesis. Amino Acids. 2012;42(2-3):627-40.
36. Chen L, Li B, Yang WC, He JL, Li NY, Hu J, et al. A dominant CD4(+) T-cell response to Helicobacter pylori reduces risk for gastric disease in humans. Gastroenterology. 2013;144(3):591-600.
37. Alexander KL, Targan SR, Elson CO, 3rd. Microbiota activation and regulation of innate and adaptive immunity. Immunol Rev. 2014;260(1):206-20.
38. Stevanović S, Pasetto A, Helman SR, Gartner JJ, Prickett TD, Howie B, et al. Landscape of immunogenic tumor antigens in successful immunotherapy of virally induced epithelial cancer. Science. 2017;356(6334):200-5.
39. Barrozo RM, Hansen LM, Lam AM, Skoog EC, Martin ME, Cai LP, et al. CagY Is an Immune-Sensitive Regulator of the Helicobacter pylori Type IV Secretion System. Gastroenterology. 2016;151(6):1164-75.e3.
40. Philip M, Schietinger A. CD8(+) T cell differentiation and dysfunction in cancer. Nat Rev Immunol. 2021.
41. Sharma P, Allison JP. Dissecting the mechanisms of immune checkpoint therapy. Nat Rev Immunol. 2020;20(2):75-6.
42. Leko V, Rosenberg SA. Identifying and Targeting Human Tumor Antigens for T Cell-Based Immunotherapy of Solid Tumors. Cancer Cell. 2020;38(4):454-72.
43. June CH, Sadelain M. Chimeric Antigen Receptor Therapy. N Engl J Med. 2018;379(1):64-73.
44. Romero P, Banchereau J, Bhardwaj N, Cockett M, Disis ML, Dranoff G, et al. The Human Vaccines Project: A roadmap for cancer vaccine development. Sci Transl Med. 2016;8(334):334ps9.
45. Mann TH, Kaech SM. Tick-TOX, it's time for T cell exhaustion. Nat Immunol. 2019;20(9):1092-4.
46. Han C, Yan P, He T, Cheng J, Zheng W, Zheng LT, et al. PHLDA1 promotes microglia-mediated neuroinflammation via regulating K63-linked ubiquitination of TRAF6. Brain Behav Immun. 2020;88:640-53.
47. Zhang M, Hu S, Min M, Ni Y, Lu Z, Sun X, et al. Dissecting transcriptional heterogeneity in primary gastric adenocarcinoma by single cell RNA sequencing. Gut. 2021;70(3):464-75.
48. Savas P, Virassamy B, Ye C, Salim A, Mintoff CP, Caramia F, et al. Single-cell profiling of breast cancer T cells reveals a tissue-resident memory subset associated with improved prognosis. Nat Med. 2018;24(7):986-93.
49. Clarke J, Panwar B, Madrigal A, Singh D, Gujar R, Wood O, et al. Single-cell transcriptomic analysis of tissue-resident memory T cells in human lung cancer. J Exp Med. 2019;216(9):2128-49.
50. Molodtsov AK, Khatwani N, Vella JL, Lewis KA, Zhao Y, Han J, et al. Resident memory CD8(+) Tcells in regional lymph nodes mediate immunity to metastatic melanoma. Immunity. 2021;54(9):2117-32.e7.
51. Kok L, Masopust D, Schumacher TN. The precursors of CD8(+) tissue resident memory T cells: from lymphoid organs to infected tissues. Nat Rev Immunol. 2021:1-11.
52. Hayward SL, Scharer CD, Cartwright EK, Takamura S, Li ZT, Boss JM, et al. Environmental cues regulate epigenetic reprogramming of airway-resident memory CD8(+) T cells. Nat Immunol. 2020;21(3):309-20.
53. Zaiss DMW, Gause WC, Osborne LC, Artis D. Emerging functions of amphiregulin in orchestrating immunity, inflammation, and tissue repair. Immunity. 2015;42(2):216-26.

54. Kofler DM, Marson A, Dominguez-Villar M, Xiao S, Kuchroo VK, Hafler DA. Decreased RORC-dependent silencing of prostaglandin receptor EP2 induces autoimmune Th17 cells. J Clin Invest. 2014;124(6):2513-22.
55. Jiang J, Dingledine R. Role of prostaglandin receptor EP2 in the regulations of cancer cell proliferation, invasion, and inflammation. J Pharmacol Exp Ther. 2013;344(2):360-7.

Figures

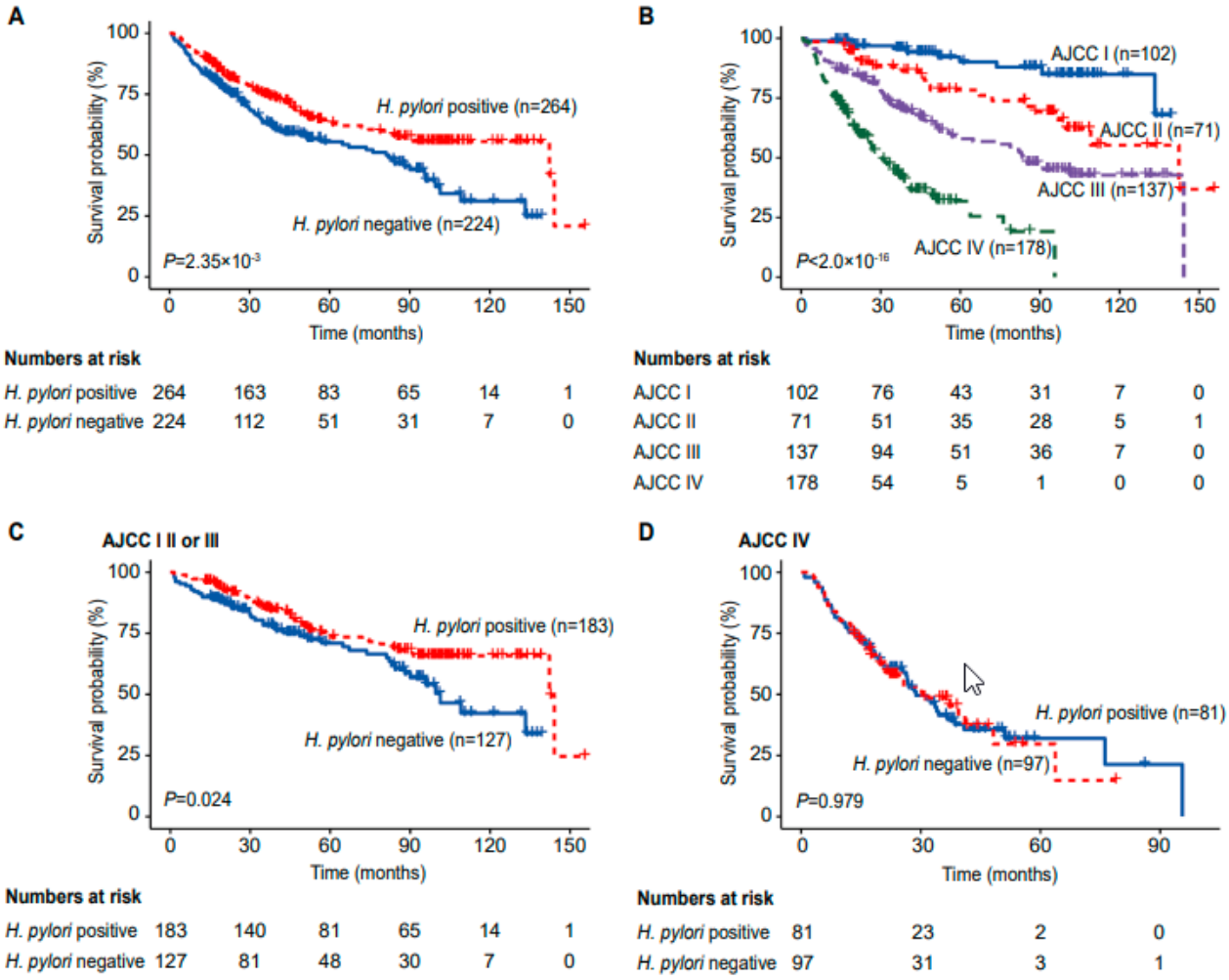

Figure 1

***H. pylori* infection was associated with better survival in Chinese gastric cancer patients. (A, B)** Kaplan-Meier survival curves for overall survival from 488 primary gastric cancer showing significant prognostic separation according to **(A)** *H. pylori* infection and **(B)** clinical stage. **(C, D)** *H. pylori* was an independent and beneficial prognostic factor pronounced in patients with **(C)** early-stage cancer, not **(D)** terminally stage cancer. *P*-value was calculated by the log-rank test.

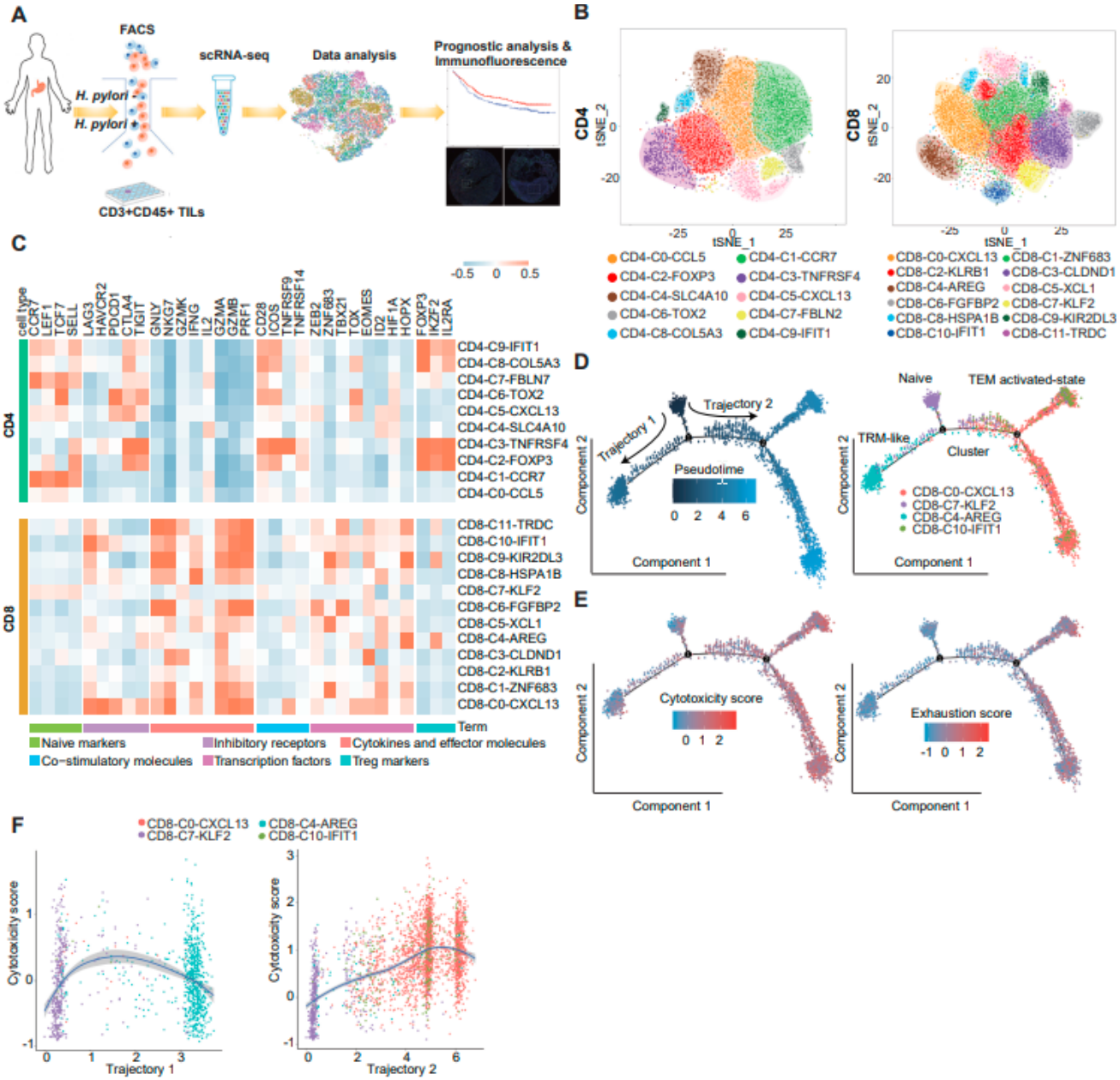

Figure 2

Dissection and identifying infiltrated cell types in gastric cancer tissues. **(A)** Workflow showing the process of sample collection, single-cell dissociation, sorting, scRNA-seq, bioinformatic analysis and validation. **(B)** Reclustering of $CD4^+$ T cell and $CD8^+$ T cells. **(C)** Average expression of selected T cell function-associated genes across different clusters. The box is proportional to the relative expression level of each gene. **(D)** The developmental trajectory of $CD8^+$ T cells inferred by Monocle2. Each dot corresponds to one single cell, colored according to its cluster label. **(E)** Monocle components were correlated with functional features of $CD8^+$ T cells, including scores of cytotoxicity and exhaustion calculated by the mean expression of gene sets related to these T cell status (see Methods). **(F)** Significantly decreased or increased score of cytotoxicity in the differentiation process colored by cell clusters. The solid lines represent the relationship between the score with Monocle components.

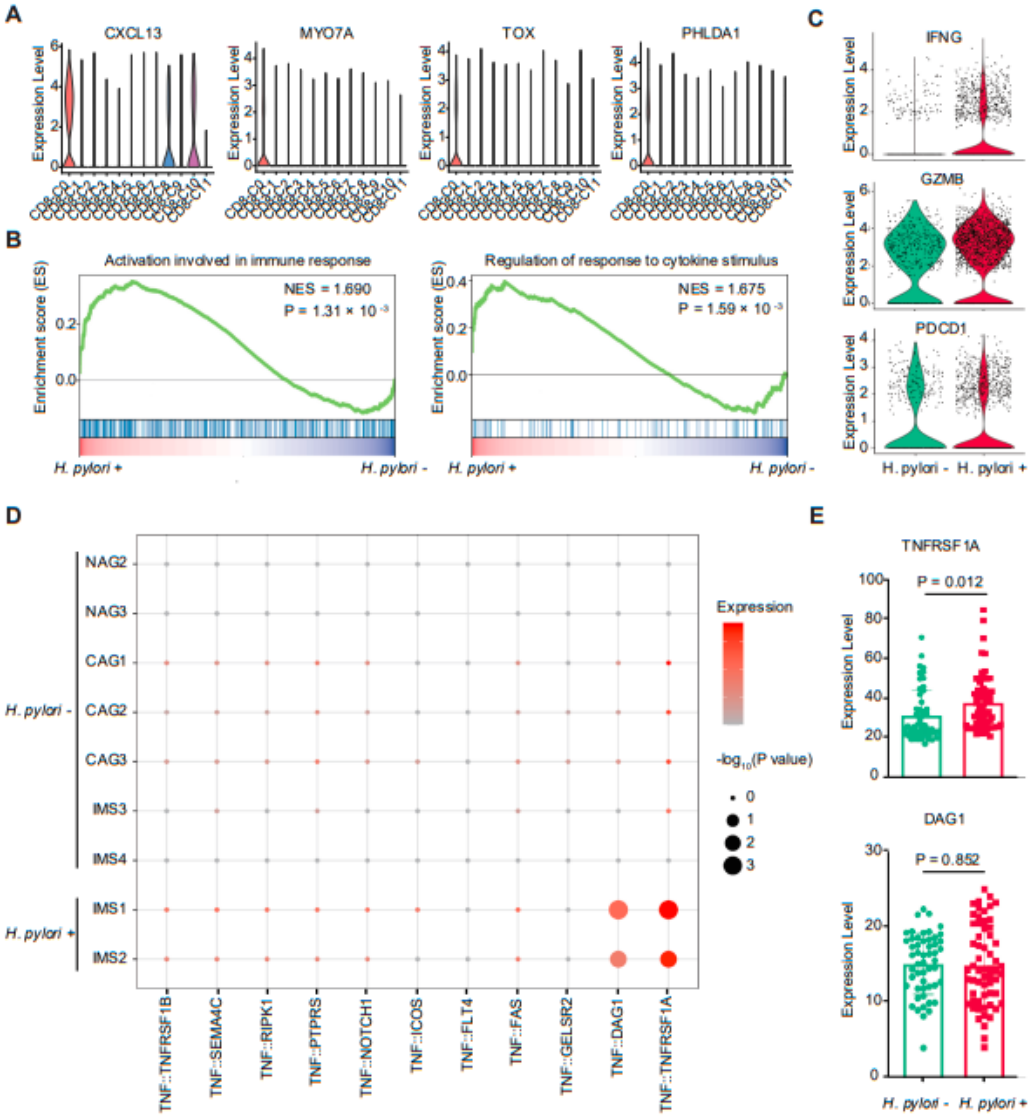

Figure 3

Detailed characterization of T cells in CD8-C0-CXCL13 cluster with different *H. pylori* infection status. (A) Violin plots showing the expression levels of genes highly expressed in T cells of CD8-C0-CXCL13 cluster. **(B)** GSEA showing top enriched pathways in *H. pylori* + derived T cells. NES denotes normalized enrichment score. **(C)** Violin plots and corresponding dots showing that the expression levels of *IFNG* and *GZMB* were upregulated, while *PDCD1* was downregulated in T cells of CD8-C0-CXCL13 cluster with *H. pylori* +. **(D)** Summary of selected ligand–receptor interactions between $CD8^+$ T cells and epithelium. *P* values (permutation test) are represented by the size of each circle. The color gradient indicates the level of interaction. **(E)** Bulk RNA sequencing data from normal gastric mucosa tissues showing that the expression of *TNFRSF1A* was significantly increased in samples with *H. pylori* infection, while *DAG1* was not changed. *P* value was calculated with student's *t* test.

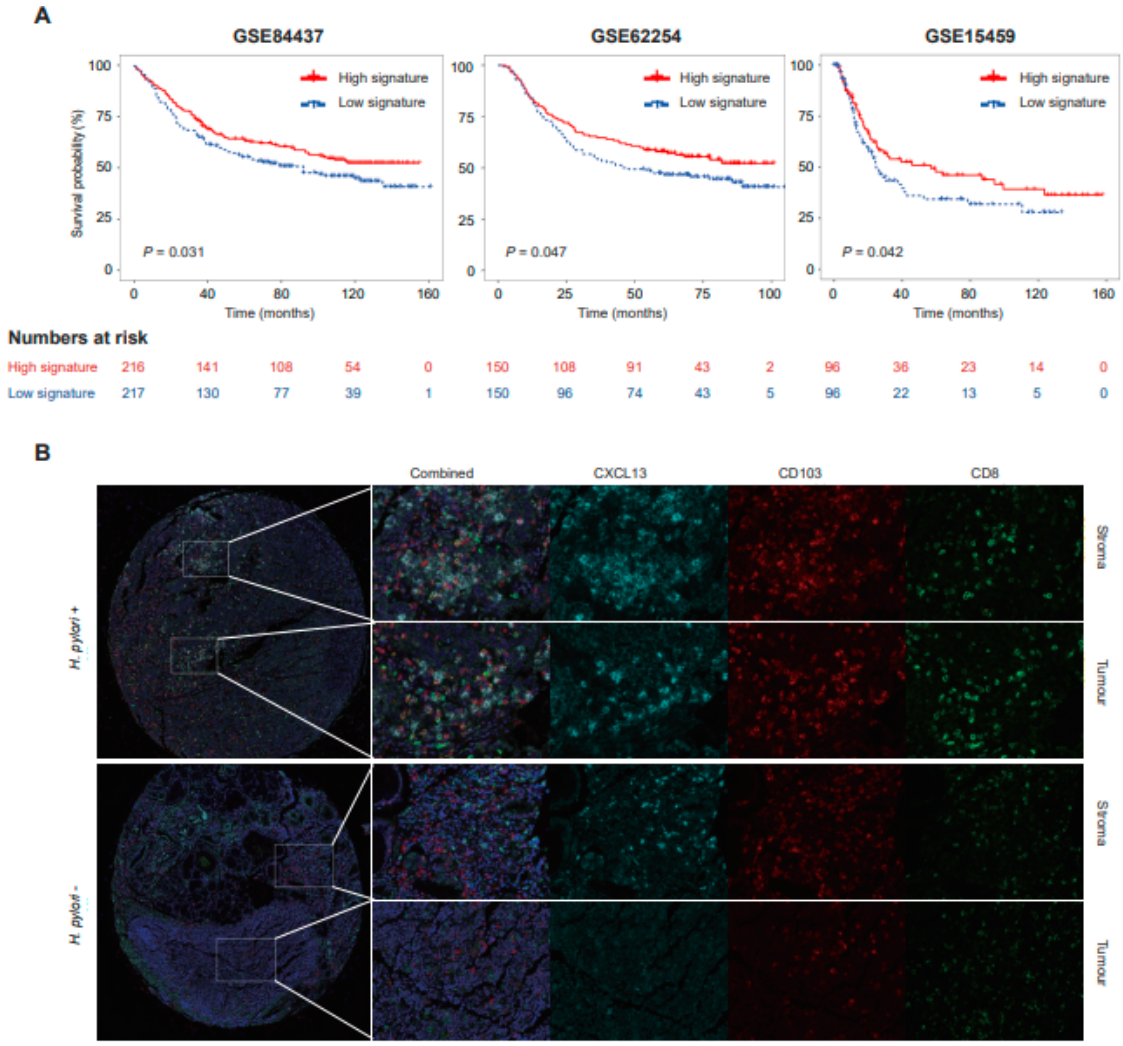

Figure 4

Prognostic abilities of the gene signature derived from single-cell data of differentially expressed genes in CD8-C0-CXCL13 for human gastric cancers. (A) Overall survival for gastric cancer patients stratified according to CD8-C0-CXCL13 signature expression. *P*-value was calculated by the log-rank test. **(B)** The multicolor immunofluorescence staining of marker genes with CXCL13, CD103 and CD8 in stroma and tumor tissues between different *H. pylori* infection status.

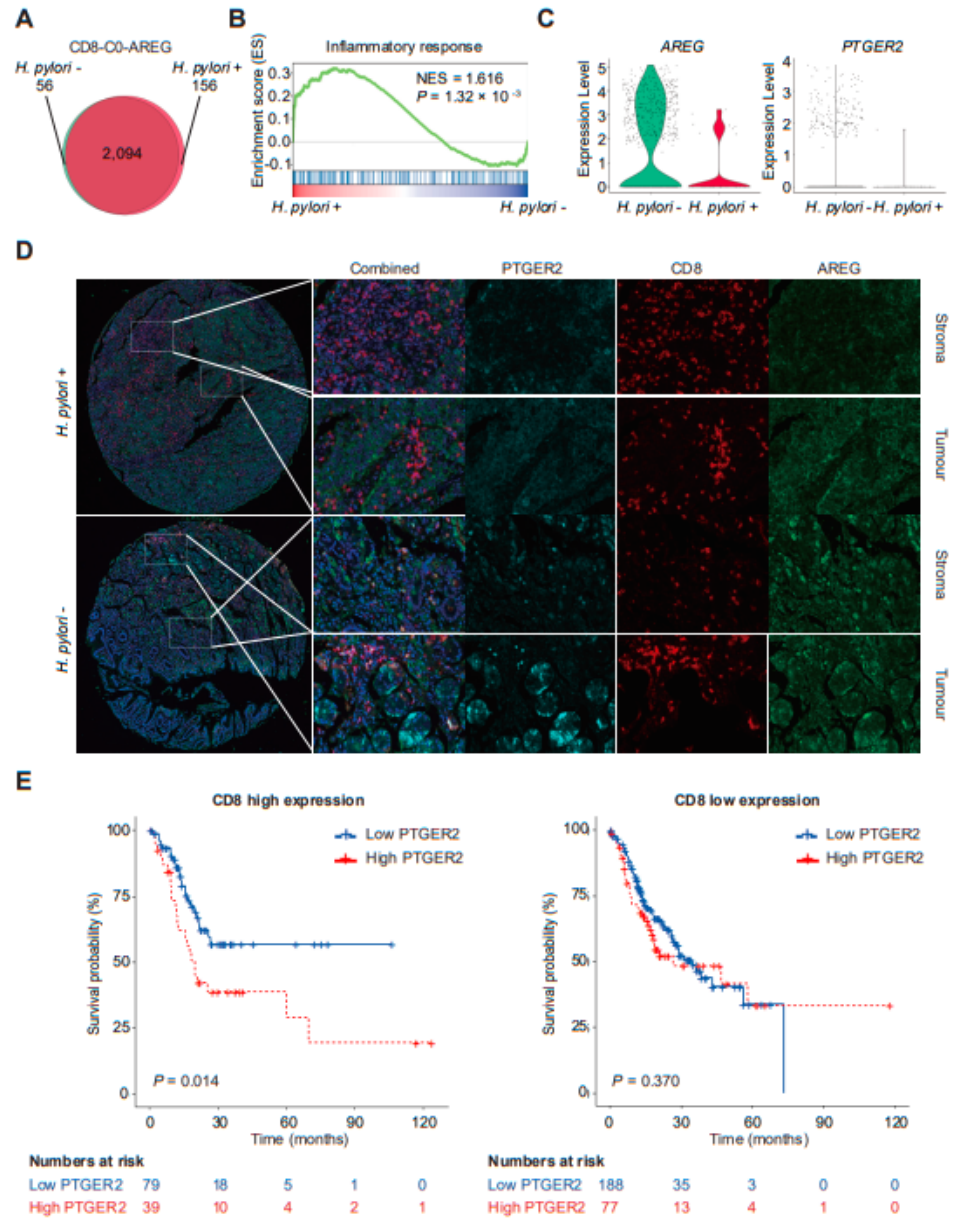

Figure 5

T_{RM} cells marked by *PTGER2* worsen prognosis in *H. pylori* negative gastric cancer. (A) Venn diagram of shared and differentially expressed genes between T cells of CD8-C4-AREG cluster from patients with different *H. pylori* infection status. **(B)** GSEA showing enriched pathways in *H. pylori* + derived T cells. NES denotes normalized enrichment score. **(C)** Violin plots and corresponding dots showing that the expression levels of *AREG* and *PTGER2* were upregulated in T cells of CD8-C4-AREG cluster with *H. pylori* -. **(D)** The multicolor immunofluorescence staining of marker genes with PTGER2, CD8 and AREG in stroma and tumor tissues between different *H. pylori* infection status. **(E)** Overall survival for gastric cancer patients further stratified according to *PTGER2* expression within *CD8* expression strata from the TCGA database. *P*-value was calculated by the log-rank test.

Supplementary Files

This is a list of supplementary files associated with this preprint. Click to download.

- supplementmaterials.pdf